Directional Solidification of Bulk (Y, Sm, Nd)$_1$Ba$_2$Cu$_3$O$_{7-x}$

M.Boffa, A.Di Trolio, S.Pace, A.Saggese and A.Vecchione
Istituto Nazionale per la Fisica della Materia and Dipartimento di Fisica Universitá di Salerno
via Salvador Allende, 84081 Baronissi (SA), Italy

B.Camarota and N.Sparvieri
CINS Alenia Direzione Ricerche, via Tiburtina km 12.4, 00131 Roma, Italy

Abstract— **Rare Earth (Nd, Sm) elements, having relatively large ionic radius, have been substituted for Yttrium in Y123 superconducting melt textured bulk samples. In (Nd, Sm)123 a wider solidification range and higher recrystallization rate than Y123 significantly increase the solidification rate, making the whole process much faster. A preliminary comparison among directionally solidified (Y, Sm, Nd)$_1$Ba$_2$Cu$_3$O$_{7-x}$ bulk bars fabricated by the Horizontal Bridgman method has been done. The different microstructural and superconducting features are studied by X-ray, SEM analysis, and ac and dc magnetic measurements. The (Nd, Sm)123 samples, appear comparable to Y123 grown with a pulling rate almost two orders of magnitude lower.**

I. Introduction

High temperature superconducting RE$_1$Ba$_2$Cu$_3$O$_{7-x}$ (123) bulk samples obtained by sintering techniques result in highly granular properties with critical current densities J_c, lower than 10^3 A/cm^2 at 77 K. On the contrary, melt texturing processes [1] are the best way to grow bulk 123 samples with reduced granularity, good texture and critical current density in excess of 10^5 A/cm^2 at 77 K.

Melt texturing processes [2], [3], start with heating of the 123 solid phase above the peritectic temperature T_p, where incongruent melting into a 211 solid and liquid phase occours. Cooling in a temperature spatial gradient G (°C/cm) through T_p at a rate R (°C/h), determines the directional solidification. The same goal can be obtained by keeping the furnace temperature profile constant in time and moving the sample. In this case the sample pulling rate R_p is directly correlated to R by the relation $R = R_p \cdot G$. In order to make a stable growth front, R_p has to be comparable to the 123 phase recrystallization rate R_g(cm/h), which directly depends on the Rare Earth (RE) diffusion rate through the liquid from 211 to 123 phases and on the RE concentration in the liquid phase. Directionally solidified YBa$_2$Cu$_3$O$_{7-x}$, doped with Y$_2$BaCuO$_5$, using an optimized R_p of the order of 0.1 cm/h, show at 77 K.a $J_c \sim 10^5$ A/cm^2 [4], [5], [6]. Unfortunately, these optimized rates make the whole fabrication process time consuming and deeply reduce the application fields for this type of compound. Significantly higher pulling rates yield only a partial 123 recrystallization, leading to a severe worsening of the superconducting properties.

It was reported [7] that the solubility of the RE in the liquid phase above T_p increases as the ionic radius of the RE atoms approaches to the size of Ba atom. The large solubility of these atoms in the melt may result in an increased concentration, which, in the presence of higher diffusivity, leads to the fast growth of 123 phase. Recently, Nd123 superconducting compound has been processed at R_p ranging from 0.1 to 20 cm/h, through a steep temperature gradient [8]. The samples obtained have a T_c onset of 93 K and a critical current at 77 K and zero applied magnetic field on the order of 5000 A/cm^2.

In the present paper, a preliminary comparison among directionally solidified (RE = Y, Sm, Nd)$_1$Ba$_2$Cu$_3$O$_{7-x}$ bulk bars is reported and the microstructural analysis is shown. The a.c. and d.c. magnetic measurements are also presented.

II. Sample Fabrication

Starting from high purity powders (99.99 %) of Y$_2$O$_3$, Nd$_2$O$_3$, Sm$_2$O$_3$ and BaCO$_3$ and CuO with a composition suitable for the fabrication of RE123 and RE211, the citrate pyrolisis modified method is used [9]. In this method, starting from the liquid nitrate solutions, homogeneous mixture with small granulometry is generated [10]. All the powders have been calcined in a furnace at 950 °C for 12 hours in air. While the oxygenation of Y123 requires an extra plateau at 550 °C for 5–7 h in O$_2$, for the (Nd, Sm)123 which has to be avoided. At the end of these steps, small bars of dimensions 50×5×5 mm^3 have been pressed using a pressure value of about 5 tons/cm^2.

The bars have been partially melted just above T_p and

Manuscript received August 25, 1996.
A. Saggese, +39 89-965-393, fax +39 89 953 804, saggese@physics.unisa.it, http://physics.unisa.it.

1051-8223/97$10.00

TABLE I
Main Fabrication Parameters

Id. sample	Stoichiometry	R_p(cm/h)	T_{max}(°C)	O_2
Y1	$YBa_2Cu_3O_{7-x}$	0.05	1200	20% [a]
Y2	$YBa_2Cu_3O_{7-x}$	0.1	1200	20% [a]
Y3	$YBa_2Cu_3O_{7-x}$	0.3	1200	20% [a]
Sm1	$SmBa_2Cu_3O_{7-x}$	0.4	1300	1% [b]
Sm2	$SmBa_2Cu_3O_{7-x}$	1.0	1300	1% [b]
Sm3	$SmBa_2Cu_3O_{7-x}$	4.0	1300	1% [b]
Nd1	$NdBa_2Cu_3O_{7-x}$	0.4	1300	1% [b]
Nd2	$NdBa_2Cu_3O_{7-x}$	1.0	1300	1% [b]
Nd3	$NdBa_2Cu_3O_{7-x}$	4.0	1300	1% [b]

[a]Oxygen percentage present in air.
[b]Oxygen percentage in an argon gas flow.

recrystallization has been performed by the Horizontal Bridgman method moving the sample in a temperature gradient. The experimental set up consists of a computer programmable step motor driving a position trasducer. By means of hollow rigid rod, the linear transducer pushes an alumina crucible containing the sample. The crucible moves with a rate R_p into the furnace. The temperature profile, determined by the maximum temperature T_{max}, is kept constant in time. The apparatus is designed to obtain R_p values ranging between 0.02 cm/h and 4 cm/h, with a spatial resolution lower than 10^{-3}mm. While the sample travels in the furnace, the local sample temperature is monitored by the presence of a thermocouple placed in the central part of the crucible and in contact with the sample center. The whole texturing process is obtained in the furnace region where the temperature is just below T_p and a gradient $G \sim 40$ °C/cm is present.

The thermal cycle details depend on the processed sample. RE123 have been prepared with a cycle consisting of a rapid heating up a value of $T > T_p$ and of a slow cooling in controlled O_2 atmosphere until the whole sample has passed through the temperature gradient. When this step is over the sample is cooled down to 550 °C at 20 °C/h . For Y123 the above processes have been performed in air (20% O_2); in contrast, a reduced O_2 partial pressure (1% concentration) is necessary for the (Nd, Sm)123 to avoid a partial substitution of Ba with the RE [11]. Y123 samples are mantained at 550 °C under a pure oxygen flow for 48 h. The Nd123 and Sm123 remain in the same conditions only for 12 h. A summary of some parameters of the texturing process, for the fabricated samples, is reported in Table 1.

III. Sample characterization

A. X-Ray and SEM Analisys.

The complete set of samples with different fabrication parameters has been characterized both with X-Ray diffraction and SEM analysis.

$\theta - 2\theta$ X-ray powder diffraction measurements have been done for all the fabricated samples. As reported in Fig.1, Y123 samples, made with the optimized R_p value, show only the 00L peaks, as in the case of well oriented materials with the c-axis orthogonal to the sample surface where the diffraction occurs. Sm123 and Nd123 samples, fabricated with R_p= 4 cm/h show also peaks different from the 00L peaks. It is believed that the presence of the other peaks is caused by the not yet optimized fabrication parameters and in particular the R_p value. However "Y123" samples fabricated with values of R_p higher than 0.5 cm/h show only a partial recrystallization of the 123 phase and the absence of any significant texture.

As far as the SEM analysis are concerned, the top image of Fig.2 shows the typical microstructure of the surface of the Y1 sample middle part. As it can be seen from the picture, there is a highly uniform zone of Y123 with light streaks lying parallel to a-b planes and to the sample pulling direction. These zones form large (roughly 1 mm^2) long-range domain alignments separated from each other by the presence of thin fissures. On the boundary of this region there is the presence of higher disordered and coarse grains of Y123 phase with small Y211 inclusions.

SEM analysis of the Sm3 sample (shown in the center image of Fig.2) reveals a quite different behaviour than the Y1 sample: in this case the streaks look like long parallel cracks on the surfaces that seems to divide the sample in strips. However, the microstructures observed are very similar to Y123 typical samples (e.g. Y2) fabricated with a not yet optimized R_p value.

Finally the bottom image of Fig.2 shows the SEM analysis of the Nd3 sample. The presence of a background texture is evident, with several deep fissures through the sample. Several imperfections cover the sample surface. These inclusions are Y123 lumps or Y211 grains. As a comparison, Y123 samples fabricated with a R_p greater than 0.5 cm/h show similar disordered structures.

B. ac Magnetic Properties

Ac magnetic measurements were carried out by means of a three coils susceptometer made of two pick-up coils opposite each other and a coaxial exciting coil powered by an ac current generator. Starting from the textured bars, samples with dimensions of about $5\times3\times2$ mm^3 were cut and placed into one of the pick-up coils in contact with a platinum thermometer. A sapphire sample holder insures thermal uniformity of the sample. Indeed, during the measurements a second thermometer monitors the

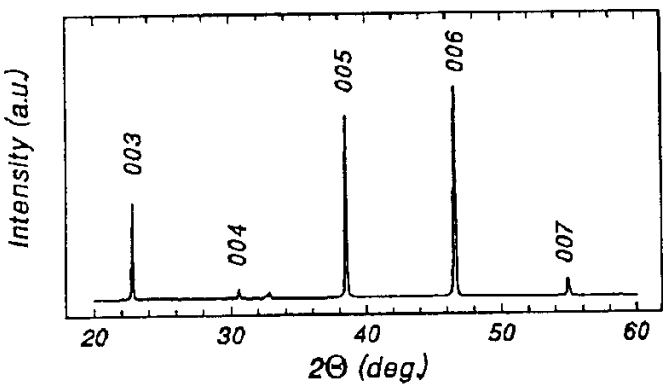

Fig. 1. X-ray diffraction pattern of the samples Y1: Only 00L peaks can be identified.

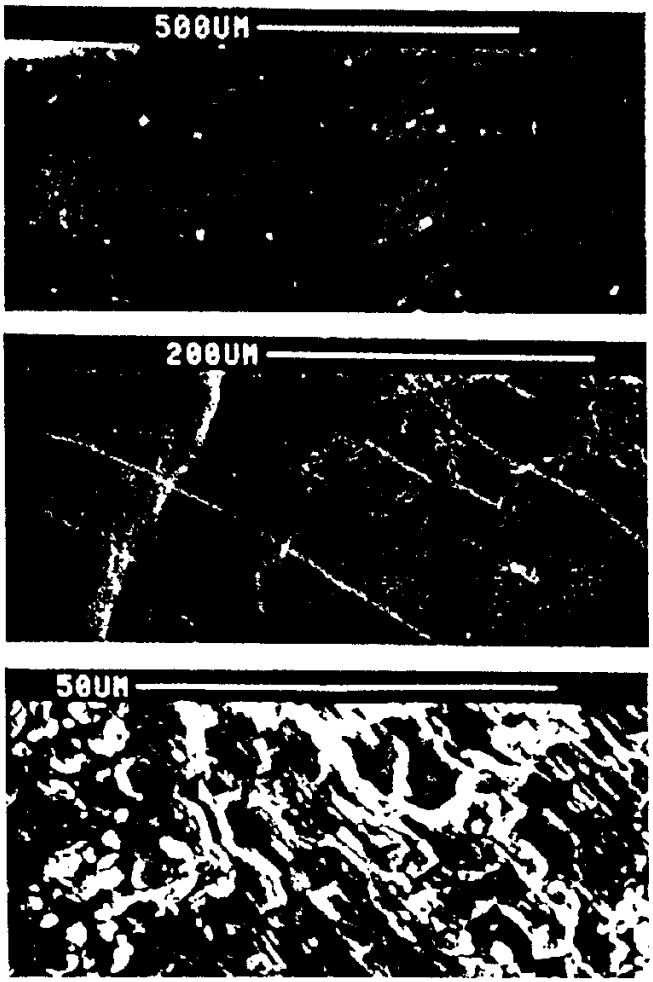

Fig. 2. Example of three pictures obtained by the SEM analisys. The Y1 sample (top), shows a high uniform zone of Y123 with light streaks. The Sm3 sample (center) shows a structure with several parallel cracks that separates uniformly grown regions. The Nd3 sample (bottom) shows only a background texture partially covered by imperfections.

temperature on the sapphire sample holder far from the sample insuring that the thermal gradient, if any, is always kept within 0.05 K. The samples were cooled down in a cryostat at about 60 K in Zero Field Cooling (ZFC) condition. After thermal stabilization, the ac magnetic field is applied and a temperature controller starts a slow ramp-up with a rate of 0.2 K/min up to 100 K.

While the temperature slowly rises, a lock-in amplifier measures the values of the in-phase and out-of-phase components of the ac voltage induced on the pick-up coils. The temperature and these voltage values are collected by a computer. The temperature dependence of the components of the real and imaginary magnetic susceptibility $\chi'(T)$ and $\chi''(T)$ are obtained after the normalization of both the in-phase and out-of-phase induced ac voltages.

The measures of $\chi'(T)$ and $\chi''(T)$ for the samples Y1, Nd3 and Sm3 are respectively shown in Fig.3(a) and in Fig.3(b). The transition temperatures of the Sm3 and Nd3 samples appear to be about 1 K lower than the Y1

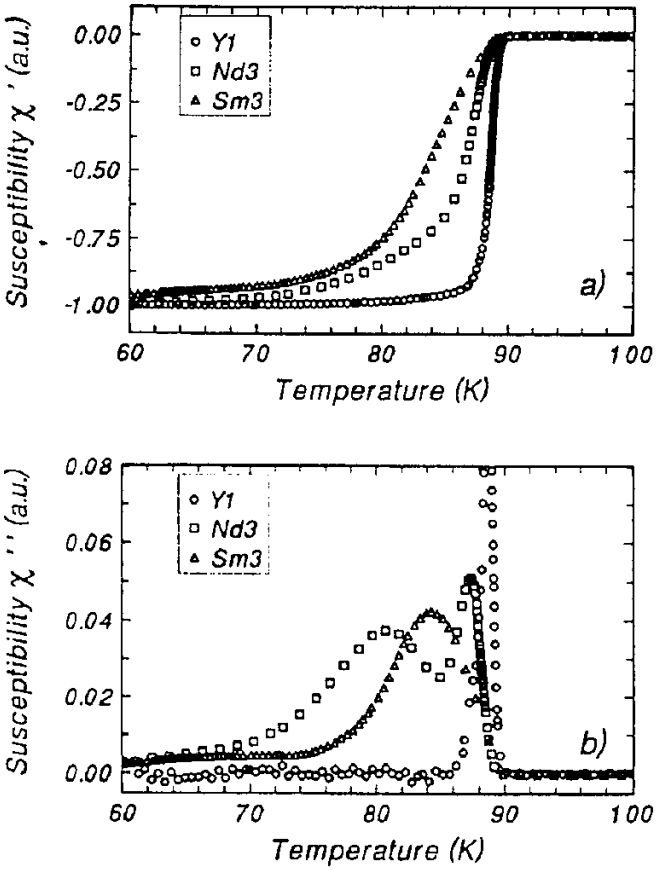

Fig. 3. In-phase χ' (a) and out-of-phase χ'' (b) low field susceptibility measurements as function of the temperature. Measurements have been done with 1 Gauss ac magnetic field at 1000 Hz.

sample. The shape of $\chi'(T)$ for the sample Y1, reported in Fig.3(a), shows a very sharp transition that is a clear indication of complete magnetic shielding. This sample, in Fig.3(b), shows a $\chi''(T)$ with a single narrow peak with a weak dependence upon the ac magnetic field, demonstrating that it is almost free from weak links.

The behaviour of $\chi'(T)$ for the Nd3 sample, shown in Fig.3(a), indicates an incomplete magnetic shielding up to the temperature of nitrogen boiling point, while $\chi''(T)$ for the same sample, reported in Fig.3(b), shows a double peak structure. Likewise sintered samples the peak at higher temperature would correspond to the losses due to the current flowing into the disjointed domains while the peak at the lower temperature would come from the losses related to the currents flowing through the weak links. This result is in agreement with the SEM analysis. Infact the picture, for this sample, reported in the previous sub-section shows the presence of thin fissures. However, the magnitude of the peak at the higher temperature is comparable to the magnitude of the Y1 peak; this feature demonstrates the presence of large grains.

The $\chi''(T)$ curve for sample Sm3, reported in Fig.3(b) shows a single broad peak. In this case, the absence of a double peak structure may be due to either a negligible contribution from intergranular shielding or to a mixing of both intergrain and intragrain losses caused by both

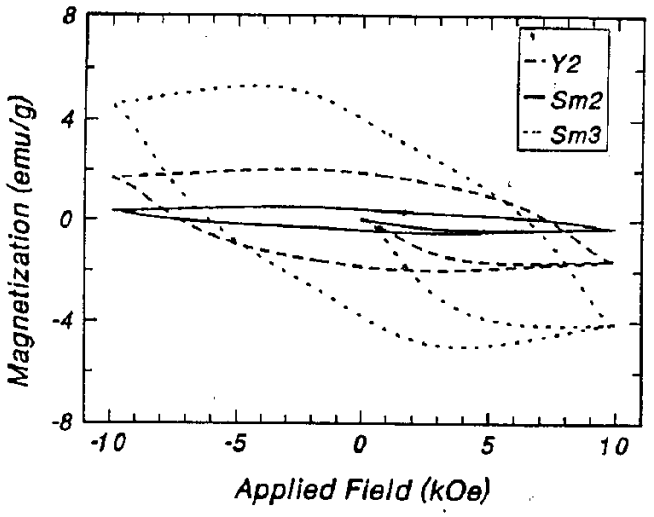

Fig. 4. M vs. H cycle for Sm2, Sm3, Y2 samples taken a T=20 K.

intergrain and intragrain critical currents on the same order of magnitude. The first hypothesis could seem the most likely since the SEM picture of this sample shows strong grain boundaries. However, in the presence of a large number of isolated grains, the magnitude of the peak should be much lower than the observed one so that the second hypothesis is actually the most probable. In this hypothesis, the Sm3 peak temperature is lower than the Y1 peak temperature, which leads to lower intergrain critical currents.

The ac susceptibility measurements, in agreement with the SEM analysis, show that the fabrication parameters for the Y1 sample and in particular the used R_p value, are optimized. The same R_p value does not optimize the fabrication process of both Sm3 and Nd3 samples. For the latter compounds the optimized fabrication processes can be obtained only by adopting higher R_p rates.

C. dc Magnetic Properties

The dc magnetization measurements were done by using a vibrating sample magnetometer EG&G PARC M4500 with an applied magnetic field perpendicular and parallel to the longitudinal axis of the bar. The applied magnetic field swung from $\pm$ 10 KOe for several values of the temperature starting from 20 K and up to liquid nitrogen temperature.

Fig.4 shows a typical hysteresis loop taken at T=20 K with the magnetic field applied perpendicularly to the pulling direction of the Sm2, Sm3 and Y2 samples. As it indicates by Fig.4, a significant improvement in the magnetization hysteresis is evident for the Sm3 sample processed with R_p value higher than Sm2 sample. However, the M-H curve of the Sm3 sample is similar to that observed on the not yet optimized Y2 sample. Moreover, for the samples shown in Fig.4, when the magnetic field was applied parallel to the sample pulling direction, only little differences in the magnetization loops were observed. Since large anisotropies in the conduction along a-b plane and c-axis direction are commonly observed from M-H loops, this result should make evident that the c-axis lies on a plane neither perpendicular nor parallel to the sample pulling direction. Hysteresis loop measurements performed on the same samples at T=77 K show a severe reduction of the dc magnetic properties.

IV. Conclusions

In this paper a comparison among textured superconducting (Y,Sm,Nd)123 samples is done. Y123 samples have a drawback of a very long crystallization time that strongly limits the potential application of those superconductors. We experienced that the substitution of Y by Nd and Sm, allows the use of a much higher pulling speed. The samples fabricated by the Horizontal Bridgman method have been characterized by X-ray diffractometry and SEM analysis and their superconducting properties were investigated by both ac susceptibility and magnetic hysteresis. The results obtained confirm that within this method it is possible to obtain samples suitable for application within reasonable process times.

References

[1] S. Jin, T. H. Tiefel, R. C. Sherwood, M. E. Davis, R. B. Van Dover, G. W. Kammlott, R. A. Fastnacht and H. D. Keith, "High critical currents in Y-Ba-Cu-O superconductors," *Appl. Phys. Lett.*, vol. 52, pp. 2074-2076, 1988.

[2] M.Murakami, "Melt process, Flux Pinning and Levitation," in *Melt processed high temperature superconductors*, M. Murakami, Ed. Singapore: World Scientific Ltd., 1992, pp. 21-44.

[3] K. Salama, V. Selvamanikam and D. F. Lee, "Melt processing and properties of Y-Ba-Cu-O," in *Processing and properties of high T_c superconductors*, vol. I,Sungho Jin, Ed. Singapore: World Scientific Ltd., 1992, pp. 155-211.

[4] B. Martinez, X. Obradors, A. Gou, V. Gomis, S. Pinol, J. Fontcuberta and H. Van Tol, "Critical currents and pinning mechanisms in directionally solidified $YBa_2Cu_3O_7$ - Y_2BaCuO_5 composites," *Phys. Rev. B*, vol. 53, pp. 2797-2809, 1996.

[5] T. Matsushita, "Critical current properties in superconducting melt processed Y-Ba-Cu-O," in *Advances in high-T_c superconductors*, vol. 137-139, 1993, pp. 677-692, .

[6] L.M. Fisher, A.V. Kalinov, J. Mirkovic and I.F. Voloshin, "Temperature and magnetic field dependencies of J_c in textured high-T_c superconductors," in *High T_c superconductors*, A. Barone, D. Fiorani and A. Tampieri, Ed. Faenza: Gruppo Editoriale Faenza Editrice S.p.A. Italy, vol. 7, 1995, pp. 99-104.

[7] Ch. Klauns, M. Sumida, M. Tagami, Y. Yamada and Y. Shiohara, "Solubility of RE elements into Ba-Cu-O melts and enthalpy of dissolution," *Zeitschrift fur Physik B*, vol. 96, pp. 207-212, 1994.

[8] K. Salama, S. Parikh and L. Woolf, "High rate melt texturing $Nd_{1-x}Ba_{2+x}Cu_3O_{7-y}$ type superconductors," *Appl. Phys. Lett.*, vol. 68, pp. 1993-1995, 1996.

[9] S. Fortunati, M. Tului and L. Risso, Ital. Pat. Appl. RM91A000555, 1991.

[10] F. Celani, A. Saggese, S: Pace, L. Liberatori and N. Sparvieri, "Bulk superconductivity on ozone annealed YBCO samples by ac screening current measurements," *Materials Chemistry and Physics*, vol. 25, pp. 43-55, 1990. (see also the Refs. 6 $\div$ 8 in this paper).

[11] S.I. Yoo, N. Sakai, H. Takaichi, T. Higuchi and M. Murakami, "Melt processing for obtaining $NdBa_2Cu_3O_y$ superconductors with high T_c and large J_c," *Appl. Phys. Lett.*, vol. 65, pp. 633-635, 1994.